Published in final edited form as:
J Bone Miner Res. 2014 December ; 29(12): 2610–2617. doi:10.1002/jbmr.2290.

Effects of Neonatal Enzyme Replacement Therapy and Simvastatin Treatment on Cervical Spine Disease in Mucopolysaccharidosis I Dogs

Joseph A Chiaro, B.S.[1,2], **Patricia O'Donnell**[3], **Eileen M Shore, Ph.D.**[2,4], **Neil R Malhotra, M.D.**[1,2], **Katherine P Ponder, M.D.**[5], **Mark E Haskins, V.M.D.**[3], and **Lachlan J Smith, Ph.D.**[1,2,*]

[1]Department of Neurosurgery, Perelman School of Medicine, University of Pennsylvania, 424 Stemmler Hall, 3450 Hamilton Walk, Philadelphia, PA, 19104, USA

[2]Department of Orthopaedic Surgery, Perelman School of Medicine, University of Pennsylvania, 424 Stemmler Hall, 3450 Hamilton Walk, Philadelphia, PA, 19104, USA

[3]Department of Pathobiology, School of Veterinary Medicine, University of Pennsylvania, 4020 Ryan Veterinary Hospital, 3900 Delancey St, Philadelphia, PA, 19104, USA

[4]Department of Genetics, Perelman School of Medicine, University of Pennsylvania, 424 Stemmler Hall, 3450 Hamilton Walk, Philadelphia, PA, 19104, USA

[5]Department of Internal Medicine, Washington University, Campus Box 8125 660 South Euclid Avenue, Saint Louis, MO, 63110, USA

Abstract

Mucopolysaccharidosis I (MPS I) is a lysosomal storage disease characterized by deficient α-L-iduronidase activity, leading to the accumulation of poorly degraded glycosaminoglycans (GAGs). Children with MPS I exhibit high incidence of spine disease, including accelerated disc degeneration and vertebral dysplasia, which in turn lead to spinal cord compression and kypho-scoliosis. In this study we investigated the efficacy of neonatal enzyme replacement therapy (ERT), alone or in combination with oral simvastatin (ERT+SIM) for attenuating cervical spine disease progression in MPS I, using a canine model. Four groups were studied: normal controls; MPS I untreated; MPS I ERT treated; and MPS I ERT+SIM treated. Animals were euthanized at one year-of-age. Intervertebral disc condition and spinal cord compression were evaluated from MRIs and plain radiographs, vertebral bone condition and odontoid hypoplasia were evaluated using microcomputed tomography, and epiphyseal cartilage to bone conversion was evaluated histologically. Untreated MPS I animals exhibited more advanced disc degeneration and more severe spinal cord compression than normal animals. Both treatment groups resulted in partial preservation of disc condition and cord compression, with ERT+SIM not significantly better than ERT alone. Untreated MPS I animals had significantly lower vertebral trabecular bone volume and mineral density, while ERT treatment resulted in partial preservation of these properties. ERT

*Correspondence: Lachlan J Smith, Ph.D., Department of Neurosurgery, Perelman School of Medicine, University of Pennsylvania, 424 Stemmler Hall, 3450 Hamilton Walk, Philadelphia, PA, 19104 USA, Ph. +1 215-746-2169, Fax. +1 215-573-2133, lachlans@mail.med.upenn.edu.

Disclosures

MEH owns stock in BioMarin Pharmaceuticals, Inc. The authors have no other disclosures relevant to this work.

+SIM treatment demonstrated similar, but not greater, efficacy. Both treatment groups partially normalized endochondral ossification in the vertebral epiphyses (as indicated by absence of persistent growth plate cartilage), and odontoid process size and morphology. These results indicate that ERT begun from a very early age attenuates the severity of cervical spine disease in MPS I, particularly for the vertebral bone and odontoid process, and that additional treatment with simvastatin does not provide a significant additional benefit over ERT alone.

Keywords

Lysosomal storage disease; Hurler Syndrome; canine model; vertebral bone; intervertebral disc; odontoid process

1. Introduction

The mucopolysaccharidoses (MPS) are a subset of lysosomal storage diseases that are characterized by deficient activity of hydrolytic enzymes that degrade glycosaminoglycans (GAGs) (1). While disease severity varies significantly depending on the specific type of MPS, manifestations can occur in the skeleton, liver, cardiopulmonary system, eyes, ears, central nervous system, and other sites. Mucopolysaccharidosis I (MPS I), also known as Hurler Syndrome, or Hurler-Scheie or Scheie Syndromes corresponding to severe, intermediate and attenuated disease phenotypes respectively, is characterized by deficient α-L-iduronidase (IDUA) activity, leading to accumulation of poorly degraded dermatan and heparan sulfate glycosaminoglycans (2). While MPS I is associated with multi-organ disease manifestations, spine disease in particular is prevalent (3,4). Surgical correction is indicated in around ~10–15% of MPS I patients as young as 4 years of age, depending on the severity of the disease (5). In the cervical spine, typical manifestations include vertebral dysplasia and subluxation, dural thickening, accelerated disc degeneration and odontoid process soft tissue hypertrophy, which are associated with spinal cord compression and/or kypho-scoliotic deformity (3,6–8). Less commonly, hypoplasia of the odontoid process may lead to atlanto-axial subluxation and spinal cord compression (3,9–12).

In our previous work using the MPS I canine model (13,14), we identified three key features of vertebral bone disease present from an early postnatal age: 1) poor trabecular bone quality (volume, architecture and mineral density); 2) hypoplasia of the odontoid process; and 3) delayed/failed cartilage to bone conversion in secondary centers of ossification (13). MPS I is also characterized by moderate to severe spinal cord compression and pathological changes to the intervertebral discs, presenting as reduced signal intensity in the central nucleus pulposus (NP) on T2-weighted magnetic resonance images (MRI) (15). While mechanisms underlying the progression of spine disease in MPS are not well understood, they likely include a combination of disruption of the signaling pathways that regulate tissue formation (16–18), and accelerated tissue destruction due to increased localized inflammation and associated protease activity (19,20). For example, the Toll-like Receptor 4 (TLR4) pathway has been implicated in the progression of inflammatory musculoskeletal disease through binding and activation by endogenous ligands, such as heparan sulfate fragments, to the TLR4 receptor (21,22).

Current treatment strategies for MPS I, including enzyme replacement therapy (ERT), hematopoietic stem cell transplantation (HSCT) and experimental gene therapy address cardiopulmonary disease manifestations, however they have demonstrated only limited efficacy in preventing the progression of spine disease (6–8,23,24), although there is evidence that higher dose or intrathecal ERT from a very early age may be more effective (15). Few studies describe the efficacy of ERT for correcting vertebral bone pathology in MPS I. A recent retrospective clinical study found that thoracolumbar kyphosis is almost universal among patients with Hurler Syndrome, despite having received an HSCT or ERT from a young age (8). While these treatments have extended the life span of MPS patients by attenuating cardiopulmonary manifestations, increased incidence of spinal problems has accompanied this increase in longevity, significantly impacting on patient quality of life. Clinical data do suggest that earlier intervention is more effective at normalizing growth and attenuating musculoskeletal disease in children with MPS I, highlighting the importance of early diagnosis (25,26). The failure of intravenous ERT to more effectively attenuate spine disease may be due in part to the large molecular weight of the enzyme (83kD), limiting its diffusion into these tissues.

One possible avenue for treating the spinal manifestations of MPS I may be to augment ERT with small molecule therapeutics that specifically target those aspects of the disease (specifically, accelerated intervertebral disc degeneration, spinal cord compression, vertebral trabecular bone quality and odontoid hypoplasia). For example, pentosan polysulfate sodium (PPS), a polysulfated polysaccharide heparin analog with anti-inflammatory and pro-chondrogenic properties, has recently shown promise for improving musculoskeletal disease in MPS VI rats (27). Simvastatin is an FDA-approved drug commonly prescribed for lowering cholesterol. It has been shown that simvastatin can both reduce inflammation by inhibiting the TLR4 signaling pathway (28,29) and stimulate bone formation by enhancing BMP2 expression (30,31), with minimal side effects.

The objective of this study was to determine the efficacy of neonatal, standard clinical dose ERT alone or in combination with oral simvastatin for attenuating cervical spine vertebral bone and intervertebral disc disease severity in MPS I in a canine model.

Materials and Methods

Animals and Treatments

Well-characterized animal models of MPS I include naturally occurring canine and feline models, and knockout murine models (32). The canine model of MPS I has a homozygous mutation in intron 1 of the IDUA gene (33), and is considered to align most closely with the intermediate severity, Hurler-Scheie phenotype seen in humans, based primarily on the pathology observed in the central nervous system, skeleton and corneas (14,34–36). Spinal manifestations in MPS I dogs show many similarities to those observed in MPS I patients. These include radiographic and gross pathological evidence of spine disease, including abnormalities of the vertebral bones, particularly in the cervical spine, frequently leading to spinal cord compression (15,37). MPS I dogs therefore represent an excellent, clinically relevant model for investigating the pathogenesis and treatment of spine disease in MPS I.

The dogs used in this study were raised at the School of Veterinary Medicine at the University of Pennsylvania, under NIH and USDA guidelines for the care and use of animals in research. MPS I-affected animals were identified at birth by DNA mutation analysis. Most normal controls were heterozygous littermates of MPS I dogs or had at least one parent in common. A total of 20 dogs were studied, divided amongst four study groups (each n=5): normal controls; MPS I untreated; MPS I ERT treated; and MPS I combined ERT and simvastatin (ERT+SIM) treated. A simvastatin only group was not included, as MPS I patients typically commence enzyme replacement therapy upon diagnosis as part of their standard of care. We therefore proposed simvastatin as an adjuvant to ERT, to target disease manifestations (i.e. musculoskeletal) that respond poorly to ERT. Treatments commenced at 1 week-of-age. Enzyme replacement therapy (recombinant human IDUA; Biomarin Pharmaceuticals; Novato, CA, USA) consisted of weekly, intravenous infusions at a dose of 0.58 mg/kg (the standard clinical dose for human patients (38)), administered over two hours. Simvastatin (Merck; Darmstadt, Germany) was administered orally once per day (2 mg/kg - the standard clinical dose range for an adult human is 20–40 mg (39)). All animals were euthanized at one year-of-age using 80 mg/kg of sodium pentobarbital in accordance with the American Veterinary Medical Association guidelines.

Magnetic Resonance Imaging and Plain Radiography

Prior to euthanasia, magnetic resonance images (MRI) and plain radiographs were obtained of the cervical spine for each animal. MR images were obtained on a 1.5T Signa LX magnet (GE Healthcare; Little Chalfont, United Kingdom). The dog was placed head first and supine in a head coil under general anesthesia. Sagittal T2-weighted images of the cervical spine were obtained using a fast recover fast spin echo sequence, with a slice thickness of 2 mm and 0.2 mm spacing, a repetition time (TR) of 3800 and an echo time (TE) of 107. A second series of images was obtained using a single shot fast spin echo sequence, with a slice thickness of 35 mm, a TR of 4000 and a TE of 1009. The final sequence included 3 separate groups of axial slices perpendicular to the spinal cord with fast recovery fast spin echoes, with a slice thickness of 3 mm and a spacing of 1 mm, with an average TR of 5000 and TE of 104. Lateral radiographs of the cervical spine were then obtained. Diagnostic reports for both MRIs and radiographs were prepared by the attending veterinary radiologist who was blinded to the treatment groups. Disc degenerative condition was assessed from MR images, independently by two blinded investigators (NRM and LJS, results averaged) using the semi-quantitative Pfirrmann grading scheme (40). Using the scheme, disc degenerative condition is assigned a score from 1 to 5 based on set morphological criteria, with a score of 1 corresponding to a healthy disc with no signs of degeneration, and 5 corresponding to a severely degenerate disc. Spinal cord compression severity was semi-quantitatively assessed from MR images using the scheme of Dickson et al (15). For this scheme, cord compression is assigned a rank from 0 to 3, according to the following criteria: 0 = absent – 360-degree cushion of CSF around the spinal cord; 1 = mild – loss of the CSF cushion without indentation of the spinal cord or only slight anterior flattening; 2 = moderate spinal cord compression; and 3 = severe spinal cord compression. Disc height index (DHI) was calculated from lateral radiographs using a custom Matlab program (41). Using this technique, disc height is normalized by the height of the two adjacent vertebral bodies, and presented as a percentage of normal. Disc condition, spinal cord compression

severity and DHI were calculated for each of 5 cervical spine levels (C2-C7). Results for individual levels were then averaged to produce single mean values for each animal. These mean values were used for subsequent statistical comparisons.

Micro-Computed Tomography (MicroCT)

Immediately following euthanasia, the cervical spine was dissected out and the C2 vertebra isolated. Vertebrae were cleaned of surrounding tissue and scanned using high-resolution microCT (VivaCT40; Scanco Medical AG, Brüttisellen, Switzerland) by our previously published methods (13). Briefly, sequential axial images through the vertebral body were obtained using an isotropic voxel size of 19 μm. Image acquisition commenced from the caudal vertebral endplate, and extended cranially for 100 slices.

Standard 3D morphometric analyses were performed using Scanco software to calculate bone volume fraction (BV/TV), trabecular thickness (Tb.Th), trabecular spacing (Tb.Sp) and trabecular number (Tb.N). Apparent mineral density (bone mineral density, BMD) was also determined and calibrated against hydroxyapatite (HA) standards (0–784 mg HA/cm^3). In additional to the trabecular bone, the entire odontoid process was imaged at the same resolution. For analyses, volumes of interest were defined as the entire structure extending from the vertebral body interface, and analyzed to determine BV/TV and BMD.

Histology

Following microCT imaging, C2 vertebral bodies were fixed in 4% paraformaldehyde for one week, then decalcified using formic acid/EDTA (Formical 2000; Decal Chemical Corporation, Tallman, USA). A 3 mm-thick mid-sagittal slab from each sample was isolated and processed for paraffin-embedded histology. Sections 10 μm thick were double-stained with Alcian blue and picrosirius red to demonstrate GAG and collagen, respectively, then imaged and analyzed under bright field light microscopy (Eclipse 90i; Nikon, Tokyo, Japan). The presence or absence of remnant growth plate cartilage in the caudal epiphysis was noted, and the total area of remnant cartilage in this region was quantified (ImageJ; National Institutes of Health, Bethesda, USA).

Statistical Analyses

Significant differences between the four study groups for measured parameters were established via 1-way ANOVAs (GraphPad Prism 5.02; GraphPad Software Inc, La Jolla, USA). Where significance was detected, post-hoc pairwise tests (Student Neumann Keuls) were performed. Differences were considered significant for $p<0.05$.

Results

MRI and Radiological Findings

A summary of findings from cervical spine MRIs and radiographs by the consultant radiologist for each individual animal are shown in Supplemental Table 1. In general, the highest incidence of abnormalities was reported for untreated MPS I animals, while normal controls had minimal abnormalities. Treated MPS I animals (both ERT and ERT+SIM) had

intermediate pathology. Of interest, abnormalities were most consistently reported at the C2–3 spine level (11 out of 20 animals).

Representative cervical spine MRIs from each group are shown in Figure 1A. With respect to semi-quantitative assessments, mean disc degenerative grade (Pfirrmann grade, Figure 1B) and spinal cord compression severity (Figure 1C) were both significantly greater for untreated MPS I animals compared to normal (both $p<0.05$), while for both ERT alone and ERT+SIM, degenerative grade and spinal cord compression severity were not significantly different from either normal or untreated (Fig 1B).

Representative lateral radiographs from each group are shown in Figure 2A. Mean DHIs for untreated MPS I animals, ERT alone and ERT+SIM were all significantly lower compared to normal ($p<0.01$, $p<0.05$ and $p<0.05$ respectively) (Figure 2B). For both ERT alone and ERT+SIM, DHI was not significantly different from untreated MPS I. For disc degenerative grade, spinal cord compression severity and DHI, ERT+SIM was not significantly better than ERT alone.

Micro Computed Tomography

For the vertebral trabecular bone (Figure 3), untreated MPS I animals had significantly rlower BV/TV (49% of normal, $p<0.001$), Tb.Th (74% of normal, $p<0.01$), Tb.N. (64% of normal, $p<0.001$) and BMD (61% of normal, $p<0.001$), and greater Tb.Sp (1.5-fold normal, $p<0.001$). Compared to untreated MPS I dogs, ERT only treated dogs had significantly greater BV/TV (85% of normal), Tb.Th (95% of normal) and BMD (89% of normal), and significantly lower Tb.Sp (1.2-fold normal), with none of these parameters significantly different from normal. ERT+SIM treatment showed similar, but not significantly greater, efficacy with respect to these parameters. Tb.N remained significantly lower than normal for both ERT only and ERT+SIM treated animals (both $p<0.001$), with neither significantly different than untreated.

Odontoid hypoplasia leading to atlanto-axial subluxation and spinal cord compression is frequently reported in children with MPS I (3,12). For untreated MPS I animals, the odontoid process was smaller than for normal animals (Figure 4A). Odontoid size was greater than untreated for both treatment groups. For untreated MPS I animals both BV/TV and BMD of the odontoid were significantly lower than normal (95% of normal for both, $p<0.05$, Figure 4B and C). For ERT, BV/TV was significantly greater than untreated MPS I ($p<0.01$), and not significantly different from normal. For ERT+SIM, BV/TV was significantly greater than both untreated MPS I and normals ($p<0.001$ and $p<0.05$, respectively). Finally, for both treatment groups, BMD was significantly greater than both untreated MPS I animals ($p<0.01$ for both) and normals (1.1-fold normal and $p<0.001$ for both).

Histology

Representative histological images of the C2 caudal epiphysis from each group are shown in Figure 5A. Large regions of remnant growth plate cartilage were observed in 4 of 5 untreated animals, 2 of 5 ERT only treated, and 2 of 5 ERT+SIM treated animals. For all other animals (in all study groups including normal controls), no or minimal growth plate

cartilage was observed. Total growth plate cartilage in the caudal vertebral epiphysis was also quantified (Figure 5B). The greatest mean cartilage area was found in untreated MPS I animals (75-fold normal), followed by ERT only treated (22-fold normal), ERT+SIM treated (5-fold normal), and normal controls, although high variability prevented differences from reaching significance.

Discussion

In this study we examined whether neonatal initiation of ERT that is administered intravenously at the standard clinical dose could prevent progressive disease manifestations in the vertebral bones and intervertebral discs of the cervical spines in MPS I. We also examined whether treatment with simvastatin could augment the therapeutic effects of ERT.

For ERT alone, partial normalization was observed with respect to vertebral trabecular bone volume, structure and BMD, odontoid process size and morphology, and in epiphyseal cartilage to bone conversion, indicative of preservation of healthy bone development relative to untreated animals. Previous studies have demonstrated that bone disease associated with MPS does respond to ERT, though with varying degrees of efficacy. Byers et al (42) examined the effects of ERT on bone formation in MPS VI (Maroteaux-Lamy Syndrome, N-acetylgalactosamine-4-sulfatase deficiency) using a feline model. Intravenous treatment beginning shortly after birth resulted in dose-dependent normalization of bone volume fraction and BMD, although even the highest dose did not restore these properties to normal levels. A recent clinical study examined the effects of ERT on three siblings with MPS I, each of whom commenced treatment at different ages and stages of disease progression (25). Results showed that treatment in the youngest child (commencing at 4 months of age) led to normalization of height and the absence of musculoskeletal disease manifestations such as joint stiffness and contractures, and facial coarsening 5 years after commencing treatment (25). In our previous work we examined the effects of neonatal retroviral gene therapy on the progression of vertebral bone disease in MPS VII (Sly Syndrome, beta-glucuronidase deficiency) (24). In this study, newborn MPS VII dogs were administered an intravenous injection of a gamma retroviral vector expressing canine beta-glucuronidase to newborn MPS VII animals, which led to transduction of liver cells and secretion of M6P-modified GUSB into blood, from where enzyme could diffuse to other organs and be taken up via the M6P receptor. This treatment led to high levels of circulating enzyme (a mean of 3.6-fold normal), however, the vertebral bone lesions were largely unresponsive. In another study MPS I dogs were treated with a retroviral vector expressing canine IDUA. At 1 year-of-age these animals exhibited attenuation of some aspects of cervical spine disease progression, including reduced incidence of vertebral widening and beaking, and intervertebral fusion (23). The results of these studies suggest that efficacy of exogenous enzyme treatment (be it by standard ERT or indirectly through RV gene therapy), may be dependent on MPS type, and the severity of the musculoskeletal phenotype (MPS VII in dogs has a more severe musculoskeletal phenotype than MPS I). In the current study, trabecular number was the only parameter to not exhibit a significant response to treatment, likely reflecting that treatments are more effective at augmenting the existing trabecular network, rather than creating entirely new trabecular elements, which is consistent with other recent findings (43).

We also examined the effects of ERT on intervertebral disc condition and spinal cord compression. Dickson et al previously showed that standard dose ERT administered intravenously from birth in MPS I dogs resulted in decreased incidence of spinal cord compression and disc degeneration compared to no treatment, although these disease manifestations were still present (15). Our results complement these findings, with partial preservation of disc health, spinal cord compression severity, and disc height index.

The drug simvastatin is widely prescribed for treatment of high cholesterol, due to its inhibition of the reductase 3-hydroxy-3-methylglutaryl-coenzyme A (HMG-CoA) (30). Simvastatin has also been widely reported to have bone anabolic properties through a variety of mechanisms, including enhanced osteogenesis by increasing the expression of BMP-2, as well as inhibition of osteoblast apoptosis and osteoclastogenesis (44). Human and murine osteoblasts exposed to statins show enhanced expression of BMP-2 mRNA, and rats treated orally with simvastatin have enhanced trabecular bone volume (30). In dogs with osteonecrosis of the femoral head, treatment with simvastatin led to significant improvements in bone structure and mineral content (45). In our study the bone anabolic effects of simvastatin in combination with ERT were not significantly different compared to ERT alone. The efficacy of ERT on its own for preventing progression of the bone pathology may potentially have masked the effects of simvastatin. Inflammation has previously been implicated in the progression of intervertebral disc disease in MPS (20). Simvastatin has also been reported to have anti-inflammatory properties through inhibition of the TLR4 signaling pathway (29). Our findings indicate that treating with both ERT and simvastatin, compared to ERT alone, did not provide a significant additional benefit in slowing the progression of disc degeneration and associated spinal cord compression, although an increased sample size and additional mechanistic studies may be required to confirm this.

Hypoplasia of the odontoid process, widely reported in MPS children, has been implicated in the high incidence of spinal cord compression in these patients (3,12). In a previous study, we described morphological abnormalities of the odontoid in MPS I dogs from as early as 3 months-of-age (13). In this study, both ERT and ERT+SIM treatment groups exhibited qualitative improvements in odontoid process size and morphology relative to untreated MPS I animals, and significant improvements in BV/TV and BMD.

In conclusion, the results of this study demonstrate neonatal ERT effectively attenuates aspects of cervical spine disease in MPS I, particularly in the vertebral bone and odontoid process. Treating with both ERT and simvastatin was found to have no statistically significant additional benefit over ERT alone. Previous animal studies and clinical case reports indicate that commencement of treatment at later stages of disease progression is likely to be far less effective than neonatal treatment, emphasizing the importance of early diagnosis and intervention (15,25,26). In our ongoing work we are seeking to further elucidate the underlying mechanisms of spine disease in MPS, with a particular emphasis on dysregulation of the signaling pathways that regulate bone development. Our long term goal is to identify new therapeutic targets for bone and disc disease in MPS, which will be effective at both early and late stages of disease progression.

Supplementary Material

Refer to Web version on PubMed Central for supplementary material.

Acknowledgments

This work was supported by grants from the Penn Center for Orphan Disease Research and Therapy (MPS I-11-007-01), the NIH (R01DK066448 and P40OD010939), and the Penn Center for Musculoskeletal Disorders (P30AR050950). Author contributions to this study were as follows: LJS and JAC contributed to conceptual design, performed experiments and drafted the manuscript; PO cared for animals and administered treatments, and critically revised the manuscript for important intellectual content; NRM performed radiological evaluations and critically revised the manuscript for important intellectual content; MEH contributed to conceptual design, supervised raising of the animals, performed post-mortems and critically revised the manuscript for important intellectual content; EMS and KPP contributed to conceptual design and critically revised the manuscript for important intellectual content. All authors approved the final version of the manuscript prior to submission. The authors would like to thank Mr John Martin for providing the custom program used to calculate DHI.

References

1. Neufeld, EF.; Muenzer, J. The Mucopolysaccharidoses. In: Scriver, CR.; Beaudet, AL.; Sly, WS.; Valle, D., editors. The metabolic and molecular bases of inherited disease. 8. McGraw-Hill; New York: 2001. p. 3421-3452.
2. Scott HS, Bunge S, Gal A, Clarke LA, Morris CP, Hopwood JJ. Molecular genetics of mucopolysaccharidosis type I: diagnostic, clinical, and biological implications. Hum Mutat. 1995; 6(4):288–302. [PubMed: 8680403]
3. Tandon V, Williamson JB, Cowie RA, Wraith JE. Spinal problems in mucopolysaccharidosis I (Hurler syndrome). J Bone Joint Surg Br. 1996; 78(6):938–44. [PubMed: 8951011]
4. White KK. Orthopaedic aspects of mucopolysaccharidoses. Rheumatology. 2011; 50(Suppl 5):v26–33. [PubMed: 22210667]
5. Arn P, Wraith JE, Underhill L. Characterization of surgical procedures in patients with mucopolysaccharidosis type I: findings from the MPS I Registry. J Pediatr. 2009; 154(6):859–64. [PubMed: 19217123]
6. Kachur E, Del Maestro R. Mucopolysaccharidoses and spinal cord compression: case report and review of the literature with implications of bone marrow transplantation. Neurosurgery. 2000; 47(1):223–8. discussion 228–9. [PubMed: 10917366]
7. Weisstein JS, Delgado E, Steinbach LS, Hart K, Packman S. Musculoskeletal manifestations of Hurler syndrome: long-term follow-up after bone marrow transplantation. J Pediatr Orthop. 2004; 24(1):97–101. [PubMed: 14676543]
8. Yasin MN, Sacho R, Oxborrow NJ, Wraith JE, Williamson JB, Siddique I. Thoracolumbar kyphosis in treated mucopolysaccharidosis 1 (hurler syndrome). Spine (Phila Pa 1976). 2014; 39(5):381–7. [PubMed: 24573070]
9. Belani KG, Krivit W, Carpenter BL, Braunlin E, Buckley JJ, Liao JC, Floyd T, Leonard AS, Summers CG, Levine S, et al. Children with mucopolysaccharidosis: perioperative care, morbidity, mortality, and new findings. J Pediatr Surg. 1993; 28(3):403–8. discussion 408–10. [PubMed: 8468655]
10. Hite SH, Peters C, Krivit W. Correction of odontoid dysplasia following bone-marrow transplantation and engraftment (in Hurler syndrome MPS 1H). Pediatr Radiol. 2000; 30(7):464–70. [PubMed: 10929365]
11. Miebach E, Church H, Cooper A, Mercer J, Tylee K, Wynn RF, Wraith JE. The craniocervical junction following successful haematopoietic stem cell transplantation for mucopolysaccharidosis type I H (Hurler syndrome). J Inherit Metab Dis. 2011; 34(3):755–61. [PubMed: 21416193]
12. Thomas SL, Childress MH, Quinton B. Hypoplasia of the odontoid with atlanto-axial subluxation in Hurler's syndrome. Pediatr Radiol. 1985; 15(5):353–4. [PubMed: 3929221]

13. Chiaro JA, Baron MD, Del Alcazar CM, O'Donnell P, Shore EM, Elliott DM, Ponder KP, Haskins ME, Smith LJ. Postnatal progression of bone disease in the cervical spines of mucopolysaccharidosis I dogs. Bone. 2013; 55(1):78–83. [PubMed: 23563357]
14. Spellacy E, Shull RM, Constantopoulos G, Neufeld EF. A canine model of human alpha-L-iduronidase deficiency. Proceedings of the National Academy of Sciences of the United States of America. 1983; 80(19):6091–5. [PubMed: 6412235]
15. Dickson PI, Hanson S, McEntee MF, Vite CH, Vogler CA, Mlikotic A, Chen AH, Ponder KP, Haskins ME, Tippin BL, Le SQ, Passage MB, Guerra C, Dierenfeld A, Jens J, Snella E, Kan SH, Ellinwood NM. Early versus late treatment of spinal cord compression with long-term intrathecal enzyme replacement therapy in canine mucopolysaccharidosis type I. Molecular Genetics & Metabolism. 2010; 101(2–3):115–22. [PubMed: 20655780]
16. Clarke LA. Pathogenesis of skeletal and connective tissue involvement in the mucopolysaccharidoses: glycosaminoglycan storage is merely the instigator. Rheumatology. 2011; 50(Suppl 5):v13–8. [PubMed: 22210665]
17. del Alcazar, CM.; Chiaro, JA.; Shore, EM.; Haskins, ME.; Smith, LJ. Delayed Chondrocyte Differentiation and Altered Indian Hedgehog Signaling Contribute to Failed Vertebral Bone Formation in Mucopolysaccharidosis VII. Orthopaedic Research Society; New Orleans: 2014.
18. Oussoren E, Brands MM, Ruijter GJ, der Ploeg AT, Reuser AJ. Bone, joint and tooth development in mucopolysaccharidoses: relevance to therapeutic options. Biochimica et Biophysica Acta. 2011; 1812(11):1542–56. [PubMed: 21827850]
19. Lai A, Simonaro CM, Schuchman EH, Ge Y, Laudier DM, Iatridis JC. Structural, compositional, and biomechanical alterations of the lumbar spine in rats with mucopolysaccharidosis type VI (Maroteaux-Lamy syndrome). J Orthop Res. 2013; 31(4):621–31. [PubMed: 23192728]
20. Smith LJ, Baldo G, Wu S, Liu Y, Whyte MP, Giugliani R, Elliott DM, Haskins ME, Ponder KP. Pathogenesis of lumbar spine disease in mucopolysaccharidosis VII. Molecular Genetics & Metabolism. 2012; 107(1–2):153–60. [PubMed: 22513347]
21. Simonaro CM, D'Angelo M, Haskins ME, Schuchman EH. Joint and bone disease in mucopolysaccharidoses VI and VII: Identification of new therapeutic targets and biomarkers using animal models. Pediat Res. 2005; 57(5 Pt 1):701–7. [PubMed: 15746260]
22. Simonaro CM, Ge Y, Eliyahu E, He X, Jepsen KJ, Schuchman EH. Involvement of the Toll-like receptor 4 pathway and use of TNF-alpha antagonists for treatment of the mucopolysaccharidoses. Proceedings of the National Academy of Sciences of the United States of America. 2010; 107(1): 222–7. [PubMed: 20018674]
23. Herati RS, Knox VW, O'Donnell P, D'Angelo M, Haskins ME, Ponder KP. Radiographic evaluation of bones and joints in mucopolysaccharidosis I and VII dogs after neonatal gene therapy. Molecular Genetics & Metabolism. 2008; 95(3):142–51. [PubMed: 18707908]
24. Smith LJ, Martin JT, O'Donnell P, Wang P, Elliott DM, Haskins ME, Ponder KP. Effect of neonatal gene therapy on lumbar spine disease in mucopolysaccharidosis VII dogs. Molecular Genetics & Metabolism. 2012; 107(1–2):145–52. [PubMed: 22510705]
25. Laraway S, Breen C, Mercer J, Jones S, Wraith JE. Does early use of enzyme replacement therapy alter the natural history of mucopolysaccharidosis I? Experience in three siblings. Molecular Genetics & Metabolism. 2013; 109(3):315–6. [PubMed: 23721889]
26. Muenzer J. Early initiation of enzyme replacement therapy for the mucopolysaccharidoses. Molecular Genetics & Metabolism. 2014; 111(2):63–72. [PubMed: 24388732]
27. Schuchman EH, Ge Y, Lai A, Borisov Y, Faillace M, Eliyahu E, He X, Iatridis J, Vlassara H, Striker G, Simonaro CM. Pentosan polysulfate: a novel therapy for the mucopolysaccharidoses. PLoS ONE [Electronic Resource]. 2013; 8(1):e54459.
28. Hodgkinson CP, Ye S. Statins inhibit toll-like receptor 4-mediated lipopolysaccharide signaling and cytokine expression. Pharmacogenet Genomics. 2008; 18 (9):803–13. [PubMed: 18698233]
29. Methe H, Kim JO, Kofler S, Nabauer M, Weis M. Statins decrease Toll-like receptor 4 expression and downstream signaling in human CD14+ monocytes. Arteriosclerosis, Thrombosis & Vascular Biology. 2005; 25(7):1439–45.

30. Mundy G, Garrett R, Harris S, Chan J, Chen D, Rossini G, Boyce B, Zhao M, Gutierrez G. Stimulation of bone formation in vitro and in rodents by statins. Science. 1999; 286(5446):1946–9. [PubMed: 10583956]

31. Chen PY, Sun JS, Tsuang YH, Chen MH, Weng PW, Lin FH. Simvastatin promotes osteoblast viability and differentiation via Ras/Smad/Erk/BMP-2 signaling pathway. Nutr Res. 2010; 30(3): 191–9. [PubMed: 20417880]

32. Haskins M, Casal M, Ellinwood NM, Melniczek J, Mazrier H, Giger U. Animal models for mucopolysaccharidoses and their clinical relevance. Acta Paediatr Suppl. 2002; 91(439):88–97. [PubMed: 12572849]

33. Menon KP, Tieu PT, Neufeld EF. Architecture of the canine IDUA gene and mutation underlying canine mucopolysaccharidosis I. Genomics. 1992; 14(3):763–8. [PubMed: 1339393]

34. Constantopoulos G, Shull RM, Hastings N, Neufeld EF. Neurochemical characterization of canine alpha-L-iduronidase deficiency disease (model of human mucopolysaccharidosis I). J Neurochem. 1985; 45(4):1213–7. [PubMed: 3928817]

35. Shull RM, Helman RG, Spellacy E, Constantopoulos G, Munger RJ, Neufeld EF. Morphologic and biochemical studies of canine mucopolysaccharidosis I. Am J Pathol. 1984; 114(3):487–95. [PubMed: 6320652]

36. Shull RM, Walker MA. Radiographic findings in a canine model of mucopolysaccharidosis I. Changes associated with bone marrow transplantation. Invest Radiol. 1988; 23(2):124–30. [PubMed: 3125125]

37. Herati RS, Knox VW, O'Donnell P, D'Angelo M, Haskins ME, Ponder KP. Radiographic evaluation of bones and joints in mucopolysaccharidosis I and VII dogs after neonatal gene therapy. Mol Genet Metab. 2008; 95(3):142–51. [PubMed: 18707908]

38. Wraith JE, Clarke LA, Beck M, Kolodny EH, Pastores GM, Muenzer J, Rapoport DM, Berger KI, Swiedler SJ, Kakkis ED, Braakman T, Chadbourne E, Walton-Bowen K, Cox GF. Enzyme replacement therapy for mucopolysaccharidosis I: a randomized, double-blinded, placebo-controlled, multinational study of recombinant human alpha-L-iduronidase (laronidase). J Pediatr. 2004; 144(5):581–8. [PubMed: 15126990]

39. Plosker GL, McTavish D. Simvastatin. A reappraisal of its pharmacology and therapeutic efficacy in hypercholesterolaemia. Drugs. 1995; 50(2):334–63. [PubMed: 8521762]

40. Pfirrmann CW, Metzdorf A, Zanetti M, Hodler J, Boos N. Magnetic resonance classification of lumbar intervertebral disc degeneration. Spine (Phila Pa 1976). 2001; 26(17):1873–8. [PubMed: 11568697]

41. Martin JT, Gorth DJ, Beattie EE, Harfe BD, Smith LJ, Elliott DM. Needle puncture injury causes acute and long-term mechanical deficiency in a mouse model of intervertebral disc degeneration. J Orthop Res. 2013; 31(8):1276–82. [PubMed: 23553925]

42. Byers S, Nuttall JD, Crawley AC, Hopwood JJ, Smith K, Fazzalari NL. Effect of enzyme replacement therapy on bone formation in a feline model of mucopolysaccharidosis type VI. Bone. 1997; 21(5):425–31. [PubMed: 9356736]

43. Altman AR, Tseng WJ, de Bakker CM, Huh BK, Chandra A, Qin L, Liu XS. A closer look at the immediate trabecula response to combined parathyroid hormone and alendronate treatment. Bone. 2014; 61C:149–157. [PubMed: 24468717]

44. Zhang Y, Bradley AD, Wang D, Reinhardt RA. Statins, bone metabolism and treatment of bone catabolic diseases. Pharmacol Res. 2014

45. Bowers JR, Dailiana ZH, McCarthy EF, Urbaniak JR. Drug therapy increases bone density in osteonecrosis of the femoral head in canines. J Surg Orthop Adv. 2004; 13(4):210–6. [PubMed: 15691182]

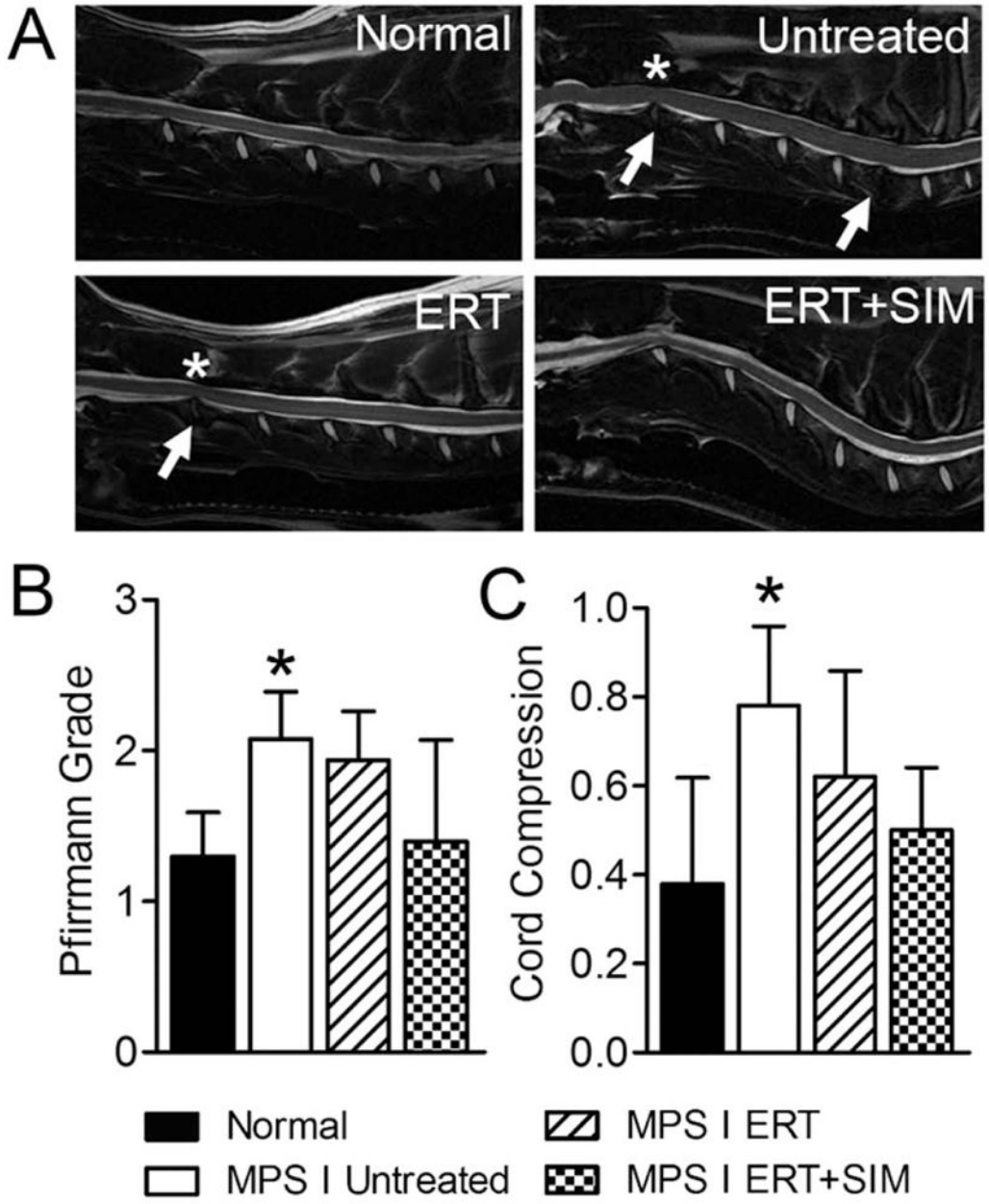

Figure 1. Magnetic resonance images were obtained for all animals prior to euthanasia at one year-of-age, and analyzed to determine intervertebral disc condition and spinal cord compression severity

A. Representative mid-sagittal, cervical spine magnetic resonance images for each study group. Arrows = examples of degenerate discs and asterisks = examples of spinal cord compression. **B.** Intervertebral disc degenerative condition (Pfirrmann grades, mean of all levels C2-C7 for each animal). **C.** Spinal cord compression severity (mean of all levels C2–C7 for each animal). *p<0.05 vs normal.

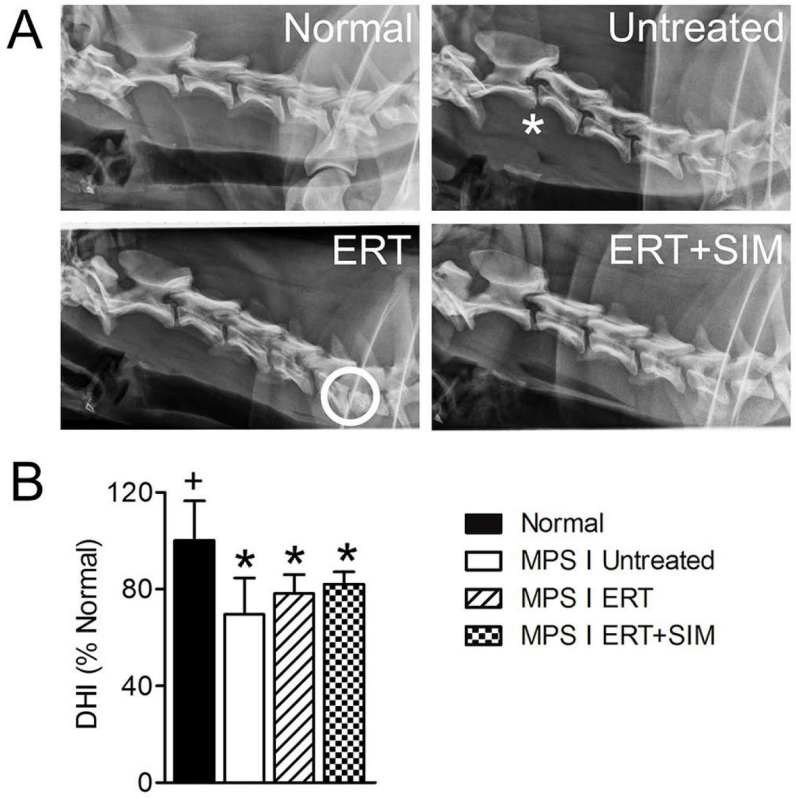

Figure 2. Lateral plain radiographs were obtained for all animals prior to euthanasia at one year-of-age, and analyzed to determine disc height index (DHI)

A. Representative lateral radiographs of the cervical spine for each study group. Asterisk = example of vertebral subluxation and circle = example of collapsed disc space. **B.** Percent change in DHI calculated from lateral plain radiographs (mean of all levels C2–C7 for each animal). *p<0.05 vs normal; +p<0.05 vs untreated MPS I.

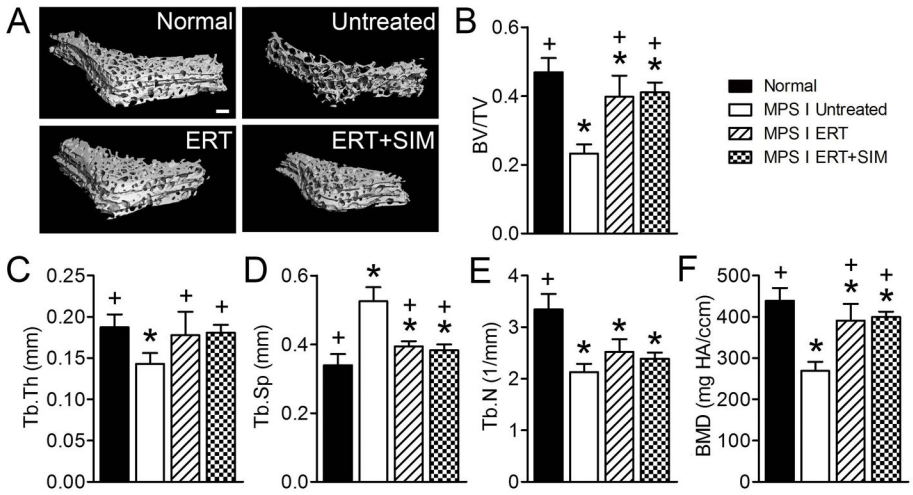

Figure 3. C2 vertebral trabecular bone was imaged post-mortem using microCT

A. Representative microCT reconstructions of C2 vertebral trabecular bone. **B.** Bone volume/total volume (BV/TV). **C.** Trabecular thickness (Tb.Th). **D.** Trabecular spacing (Tb.Sp). **E.** Trabecular number (Tb.N). **F.** Bone mineral density (apparent density, BMD). *p<0.05 vs normal; +p<0.05 vs untreated MPS I.

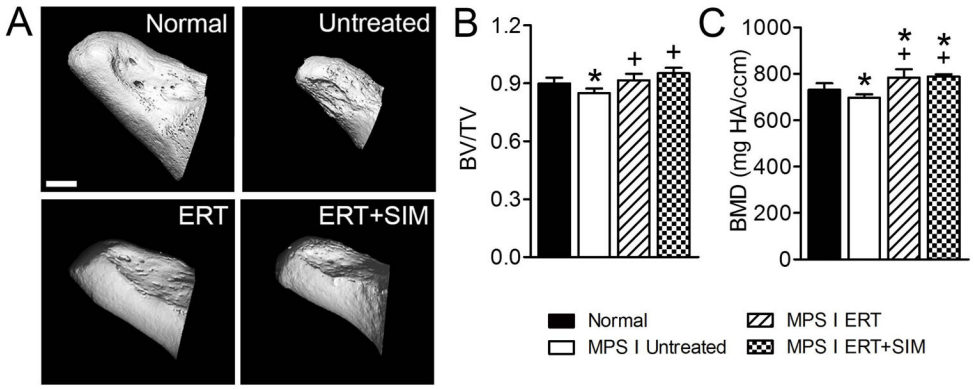

Figure 4. The odontoid process was imaged post mortem using microCT

A. Representative microCT reconstructions of the odontoid process. **B.** Bone volume/total volume (BV/TV). **C.** Trabecular thickness (Tb.Th). **D.** Trabecular spacing (Tb.Sp). **E.** Trabecular number (Tb.N). **F.** Bone mineral density (apparent density, BMD). *p<0.05 vs normal; +p<0.05 vs untreated MPS I.

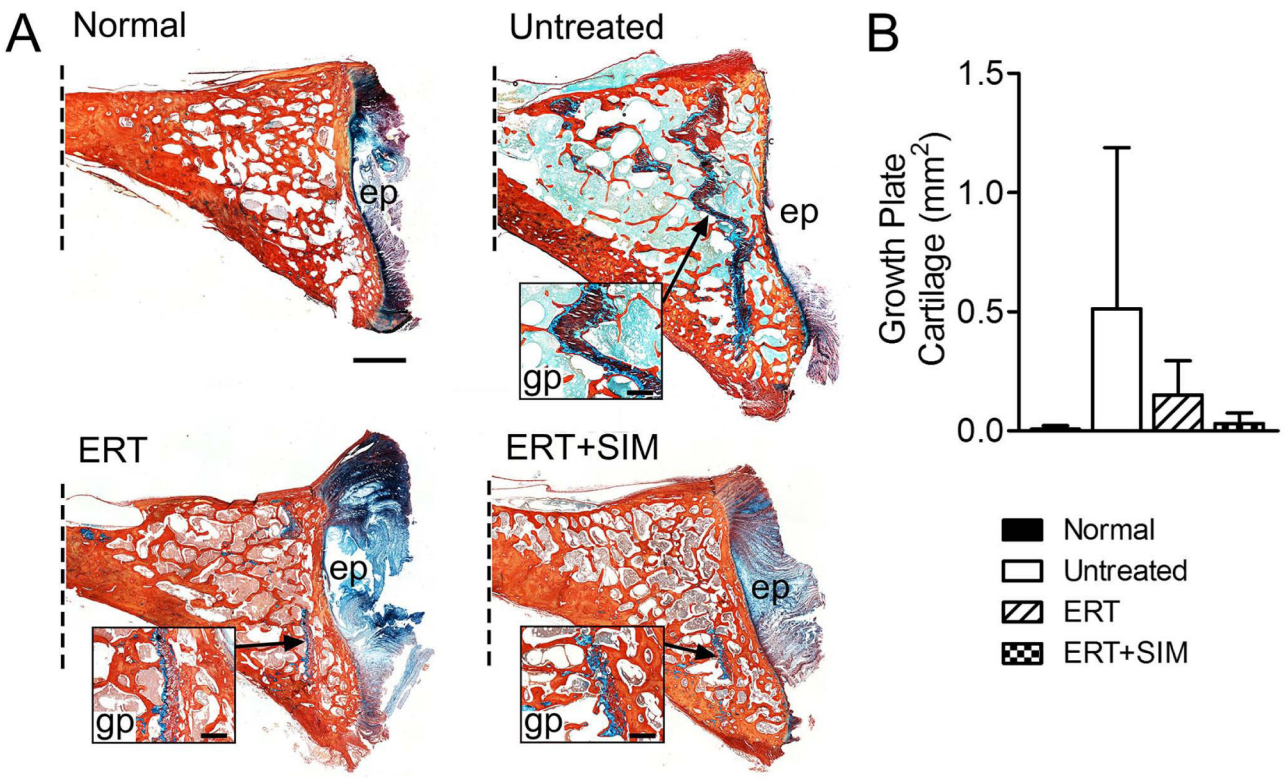

Figure 5. C2 vertebral bodies were processed for histological assessment of remnant growth plate cartilage

A. Representative histology illustrating remnant growth plate cartilage (insets) in the caudal epiphyses of C2 vertebral bodies (Alcian blue (GAG)/picrosirius red (collagen) stained mid-sagittal sections, oriented with dorsal at the top; dotted line indicates where the image is truncated in the cranial direction). Scale bar = 2mm (main images) and 1mm (insets); ep = vertebral end plate, gp = growth plate. **B**. Quantification of remnant growth plate cartilage area (mm^2) in each study group.